Blood Cells, Molecules, and Diseases (2001) **27**(1) Jan/Feb: 143–147
doi:10.1006/bcmd.2000.0367, available online at http://www.idealibrary.com on IDEAL®

Single-Particle Tracking and Laser Optical Tweezers Studies of the Dynamics of Individual Protein Molecules in Membranes of Intact Human and Mouse Red Cells

Submitted 11/27/00
(Communicated by J. Hoffman, Ph.D., 12/02/00)

Rossen Mirchev[1,2] and David E. Golan[1,2]

INTRODUCTION

The combined use of single-particle tracking (SPT) (1) and laser optical tweezers (LOT) (2) techniques represents a powerful and novel approach to elucidation of both *the dynamic molecular interactions* and *the magnitudes of the molecular forces* that regulate cell surface protein dynamics. These techniques can be applied to study membrane structure (e.g., interactions between transmembrane proteins and membrane skeletal proteins) and membrane function (e.g., cell–cell adhesion, cell activation, endocytosis, and cell signaling). In the SPT technique, individual molecules are observed by labeling with a gold, latex, or fluorescent marker. Computer-enhanced video microscopy is used to track the motion of the labeled molecules. The typical spatial resolution is 5–10 nm, well below the resolution limit of the light microscope, and the typical temporal resolution is 0.1–33 ms. SPT has several advantages over the fluorescence recovery after photobleaching (FRAP) technique (3) for measuring lateral diffusion rates of membrane proteins: (i) the spatial resolution of SPT is two orders of magnitude higher than that of FRAP but the temporal resolution is similar, so the minimum detectable diffusion coefficient is two orders of magnitude lower; (ii) there is no averaging over the diffusive behavior of thousands of molecules in SPT, so different subpopulations that are indistinguishable by FRAP can be resolved; and (iii) obstructions and confinements by lipid domains, the membrane skeleton, or the extracellular matrix can be observed and measured in SPT, and different modes of motion can be recognized. In this work, we describe the design and construction of a new system for SPT and LOT measurements of the dynamics of individual protein molecules in membranes of intact human and mouse red blood cells (RBCs).

METHODS

Bead–Protein Conjugation

Colloidal gold (RDI) is mixed with 3–5 μg IgG per milliliter gold at pH 9.0. After 3 min, PEG20 (Sigma) is added to a final concentration of 0.05% and mixed for 4 min. The gold is then centrifuged at 10,000*g* for 30 min, and the supernatant is discarded. The beads are resuspended in PBS with 0.02% PEG20, pH 7.4, and centrifuged for 30 min. The final suspension of gold beads is prepared such that the optical density is 4–8 at the appropriate (bead size dependent) wavelength (4). IgG is fragmented using a Fab′ preparation kit (Pierce). Fab′ fragments are conjugated to gold using the above procedure, except that the conjugation step is performed at pH 7.0. Concanavalin A (Con A)

This paper is based on a presentation at the Red Cell Club Meeting held at Yale University School of Medicine on October 14, 2000.

Correspondence and reprint requests to: David E. Golan, Department of Biological Chemistry and Molecular Pharmacology, Harvard Medical School, 250 Longwood Avenue, Boston, MA 02115. Fax: (617) 432-3833. E-mail: dgolan@hms.harvard.edu.
[1] Department of Biological Chemistry and Molecular Pharmacology, Harvard Medical School, Boston, Massachusetts 02115.
[2] Department of Medicine, Harvard Medical School and Brigham and Women's Hospital, Boston, Massachusetts 02115.

1079-9796/01 $35.00

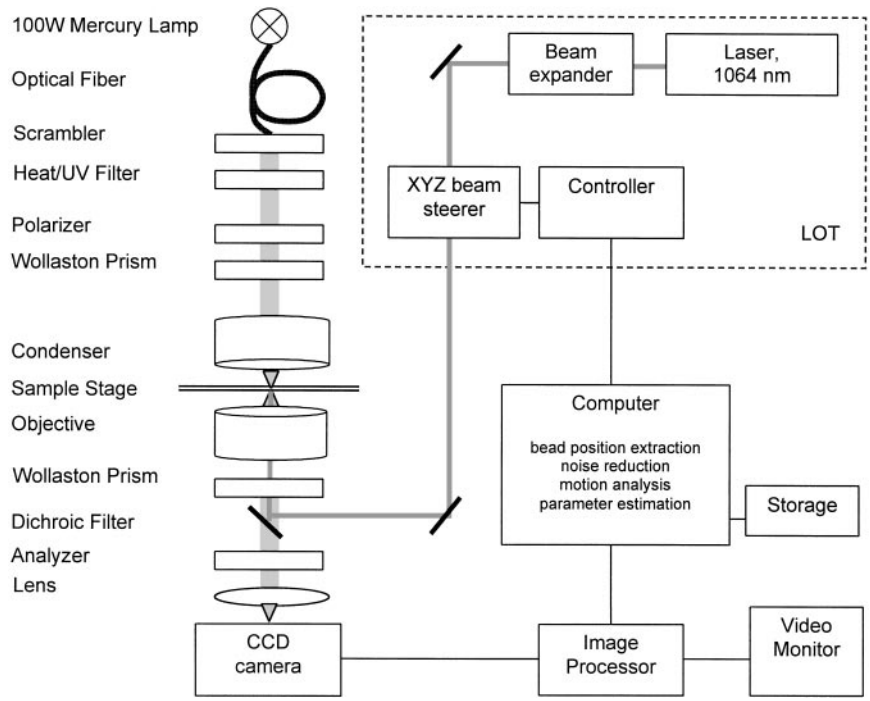

FIG. 1. Apparatus for single-particle tracking and laser optical tweezers experiments.

is coupled to gold at pH 9.0. Latex microspheres (Polysciences) are covalently conjugated to proteins, essentially as suggested by the manufacturer.

RBC Labeling

Fresh human blood (Hematology Laboratory, Brigham and Women's Hospital) is centrifuged at 1500*g* for 10 min. The plasma and buffy coat are discarded, and the RBCs are washed three more times in PBS, pH 7.4, at 500*g* for 2 min. RBCs are then resuspended to 10% hematocrit in PBS with 10 mM glucose, pH 7.4, and used in experiments within 24 h. RBCs are labeled with the conjugated beads for 40 min at room temperature with continuous mixing, then washed twice and resuspended in PBS with 1% BSA, pH 7.4. The labeled cells are placed between a microscope slide and a coverslip, and allowed to settle before viewing. To verify the specificity of labeling, control samples are prepared using beads conjugated to PEG20 only or to nonspecific IgG molecules or Fab′ fragments (see below), or RBCs are incubated with beads in the presence of agents that specifically block the binding sites of labels on the membrane protein of interest.

SPT/LOT Apparatus

The experimental apparatus is shown schematically in Fig. 1. An inverted microscope (Eclipse TE300, Nikon) is equipped with differential interference contrast (DIC) optics. Light from a 100-W mercury arc lamp is delivered by an optical fiber (Technical Video) and passed through a scrambler (Technical Video) and a filter (Omega Optical) that rejects the UV and IR wavelength regions. An oil-immersion condenser and oil-immersion 100×/1.4 NA and 60×/1.4 NA objectives are used. Images are recorded using a CCD video camera (Motion Corder Analyzer SR-Ultra, Kodak) at rates of 30 to 10,000 frames per second and transferred to a computer for storage and analysis. Tracking of bead motion is performed using the MetaMorph 3.5 software package (Universal Imaging), and the bead trajectories are analyzed using custom software. A 1064-nm Nd:YVO_4 laser (Millenia IR, Spectra Physics) provides the beam for laser tweezers experiments.

Blood Cells, Molecules, and Diseases (2001) **27**(1) Jan/Feb: 143–147
doi:10.1006/bcmd.2000.0367, available online at http://www.idealibrary.com on IDEAL®

The beam is expanded, passed through steering optics, introduced into the microscope light path using a dichroic filter (Chroma), and then focused on the sample by the objective. A motorized gimbal mirror steers the trap in the *x*- and *y*-directions in the sample plane, and a lens on a motorized linear stage moves the trap in the *z*-direction perpendicular to this plane.

Single-Particle Tracking Analysis

Single-particle trajectories are analyzed based on calculations of the mean square distance (MSD) statistic:

$$\mathrm{MSD}(\Delta t_n) = \frac{1}{N-n}\sum_{i=1}^{N-n}[(x_{i+n}-x_i)^2 + (y_{i+n}-y_i)^2], \quad [1]$$

where x_i and y_i are the coordinates of the ith position in the track, $\Delta t_n = n \times \delta$, δ is the time interval between successive images, and N is the total number of images (5). MSD(Δt_n = 1–4) can be used to estimate the diffusion coefficient of the labeled molecule over short times and distances. MSD(Δt_n = 1–4) are fitted by least-squares analysis to the general function for lateral motion:

$$\mathrm{MSD}(t) = Gt^{\alpha}, \quad [2]$$

where G and α are fitted parameters that describe the rate and type of motion (i.e., confined diffusion, Brownian diffusion, or directed motion) (6). The diffusion coefficient derived from analysis of MSD(Δt_n = 1–4), called the microdiffusion coefficient (D_μ), can be interpreted in terms of a pure diffusion process unaffected by any barriers or obstacles to lateral motion (7). In the case of pure Brownian motion, $\alpha = 1$ and D_μ = G/4. Over longer time and distance scales, the motion of the labeled molecule may be confined by barriers, such as the membrane skeleton, and/or obstacles, such as other membrane proteins or lipid rafts. MSD(Δt_n) for $n > 4$ are fitted by least squares analysis to yield the macrodiffusion coefficient, D_M. The dimensions of the confinement region in the *x*- and *y*-directions, L_x and L_y, can be estimated from nonlinear least-squares fits to the equations (8):

$$\mathrm{MSD}_x(\Delta t_n) = \frac{L_x^2}{6} - \frac{16L_x^2}{\pi^4}\sum_{n=1(\mathrm{odd})}^{\infty}\frac{1}{n^4}\exp\left[-\left(\frac{n\pi}{L_x}\right)^2 D_\mu t\right], \quad [3]$$

$$\mathrm{MSD}_y(\Delta t_n) = \frac{L_y^2}{6} - \frac{16L_y^2}{\pi^4}\sum_{n=1(\mathrm{odd})}^{\infty}\frac{1}{n^4}\exp\left[-\left(\frac{n\pi}{L_y}\right)^2 D_\mu t\right].$$

Note that the standard deviation of the MSD(Δt_n) statistic increases with n (Eq. [1]). Hence, only one-third of the time intervals in any given particle trajectory are used for the fit.

RESULTS AND DISCUSSION

Labeling

Beads are prepared by conjugating colloidal gold (20 or 40 nm in diameter) or carboxylated latex microspheres (40, 100, or 1000 nm in diameter) to monoclonal antibodies, antibody fragments, or lectins that specifically bind the membrane protein of interest. Intact IgG molecules or Fab′ fragments of monoclonal antibodies can be used. In our hands, Fab′ fragments have proven to be easier to conjugate, more efficient in binding antigens, and more convenient in preventing the cross-linking of beads to several membrane protein molecules than have intact antibodies. Two steps are taken in order to control the valency of labeling (i.e., the number of cell surface molecules labeled by a single bead). First, nonspecific IgG molecules or Fab′ fragments are mixed with the specific antibodies or antibody fragments before the antibodies or antibody fragments are conjugated to gold. Second, nonconjugated IgG molecules or Fab′ fragments are present in the solution of conjugated beads that is used to label cells. The lectin Con A is conjugated to beads without the use of nonspecific proteins.

Successful application of the SPT technique

relies on the ability to achieve an optimal number of beads bound per cell. Beads that are separated by <400 nm are optically indistinguishable, because this separation distance is below the resolution limit of the microscope. The control (i.e., nonspecifically labeled) samples show background labeling of 0–5 beads per 100 cells. Thus, highly specific labeling can be achieved using conditions that result in 1–10 beads bound per cell. It is also important to optimize the surface density of specific antibody or lectin on the bead, so as to allow specific labeling of a single cell surface molecule by a single bead, without cross-linking of multiple cell surface molecules. Experimentally, cross-linking of cell surface molecules is manifested by lateral immobilization of the bead. The fraction of immobile beads is therefore used to optimize the valency of labeling, because this fraction should equal the reported fractional mobility of the corresponding membrane protein (e.g., determined by using the FRAP technique) in the absence of cross-linking. For example, FRAP measurements show that about 40% of band 3 molecules are laterally immobile in intact normal human RBCs (9). Experimental conditions for antibody or lectin conjugation to beads are adjusted until the SPT measurements of anti-band 3–gold or Con A–gold trajectories show about 40% immobile band 3 molecules. In all cases, we use the minimum surface density of specific antibody or lectin required to achieve adequate labeling without membrane protein cross-linking. Under these conditions, the absolute values of the SPT-measured macrodiffusion coefficients are found to agree with those measured by using the FRAP technique, providing additional evidence that the beads are not cross-linking cell surface band 3 molecules.

The protocol for covalent attachment of antibodies or lectins to 1000-nm latex microspheres produces multivalent beads. Such beads can be used as a handle for pulling and holding RBCs with the laser tweezers. Monovalent 40-nm latex microspheres are used for SPT applications.

Experimental Uncertainty

Although beads less than 0.5 μm in diameter are smaller than the resolution limit of the light microscope, the image produced by such beads can be measured and followed over time. Defining the trajectory of a bead involves: first, identifying the characteristic pattern produced by the bead in the digitized image; second, determining the centroid of this characteristic pattern; third, recording the coordinates of the centroid; and fourth, proceeding to the next image in the sequence (10). This bead identification and tracking procedure introduces an error into the measurements that adds to the error due to noise in the experimental system. To estimate the experimental uncertainty inherent in SPT measurements on intact RBCs, RBCs are first labeled with beads and then fixed using glutaraldehyde. Fixation is used to produce immobile beads on the RBC surface. Under these conditions, any detectable bead movement is a result of fluctuations in the experimental SPT/LOT apparatus (including both hardware and software). Table 1 shows a series of measurements of apparent band 3 motion on glutaraldehyde-fixed human RBCs labeled with 20-nm Con A–gold beads. Two beads on each cell are tracked over time. The x and y box dimensions define the region in which each bead is localized over a period of 8 s. Using one of the beads as a reference, the relative posi-

TABLE 1

Motion of Beads Attached to Band 3 on Fixed Human RBCs

		Box dimension		SD of relative position	
	Cell No.	x (nm)	y (nm)	Δx_{rel} (nm)	Δy_{rel} (nm)
Plain glass	1	4.1	3.4	4.9	4.9
		4.2	3.8		
	2	4.3	3.9	5.2	6.0
		4.3	4.9		
	3	3.1	1.8	6.8	7.1
		6.5	7.0		
Average		3.8	3.5		
Poly-L-lysine-covered glass	4	2.4	2.8	5.3	3.1
		5.5	1.2		
	5	2.3	5.8	3.2	3.5
		2.8	7.3		
	6	11.0	9.0	10.5	7.7
		4.0	8.0		
Average		4.2	4.5		

Blood Cells, Molecules, and Diseases (2001) **27**(1) Jan/Feb: 143–147
doi:10.1006/bcmd.2000.0367, available online at http://www.idealibrary.com on IDEAL®

tions of the two beads x_{rel} and y_{rel} can also be calculated. The standard deviations Δx_{rel} and Δy_{rel} are shown in Table 1. Images are recorded every 1/125 s. The results obtained using RBCs that are allowed to settle on a plain glass cover slip are identical to those obtained using RBCs attached to poly-L-lysine coated cover slips. In both cases, the bead position is determined with $<$5-nm uncertainty.

Band 3 Diffusion in Human and Mouse RBCs

Preliminary results obtained using Con A–gold beads to label intact human and mouse RBCs show that band 3 macrodiffusion coefficients in normal RBCs are within experimental error of the FRAP-derived diffusion coefficients for band 3 in these cells. The microdiffusion coefficients are approximately 10 times greater than the macrodiffusion coefficients. The motion of the labeled proteins does not appear to be affected by the presence of the marker particles.

ACKNOWLEDGMENTS

This paper is based on a presentation given at the Red Cell Club Meeting held at Yale University School of Medicine on October 14, 2000. This work was supported by NHLBI Grants R37 HL32854 and P60 HL15157.

REFERENCES

1. Saxton, M. J., and Jacobson, K. (1997) Single-particle tracking: Application to membrane dynamics. *Annu. Rev. Biophys. Biomol. Struct.* **26,** 373–399.
2. Svoboda, K., and Block, S. M. (1994) Biological application of optical forces. *Annu. Rev. Biophys. Biomol. Struct.* **23,** 247–285.
3. Golan, D. E. (1989) Red blood cell membrane protein and lipid diffusion. *In* Red Blood Cell Membranes (Agre, P., and Parker, J. C., Eds.), pp. 367–400. Dekker, New York.
4. Leunissen, J. L. M., and De Mey, J. R. (1989) Preparation of gold probes. *In* Immunogold Labeling in Cell Biology (Verkleij, A. J., and Leunissen, J. L. M., Eds.), pp. 3–17. CRC Press, Boca Raton, FL.
5. Qian, H., Sheetz, M. P., and Elson, E. L. (1991) Single particle tracking: Analysis of diffusion and flow in two-dimensional systems. *Biophys. J.* **60,** 910–921.
6. Feder, T. J., Brust-Mascher, I., Slattery, J. P., Baird, B., and Webb, W. W. (1996) Constrained diffusion or immobile fraction on cell surfaces: A new interpretation. *Biophys. J.* **70,** 2767–2773.
7. Saxton, M. J. (1995) Single particle tracking: Effects of corrals. *Biophys. J.* **69,** 389–398.
8. Kusumi, A., Sako, Y., and Yamamoto, M. (1993) Confirmed lateral diffusion of membrane receptors as studied by single-particle tracking (nanovid microscopy). *Biophys. J.* **65,** 2021–2040.
9. Corbett, J. D., Cho, M. R., and Golan, D. E. (1994) Deoxygenation affects fluorescence photobleaching recovery measurements of red cell membrane protein lateral mobility. *Biophys. J.* **66,** 25–30.
10. Gelles, J., Schnapp, B. J., and Sheetz, M. P. (1988) Tracking kinesin-driven movements with nanometre-scale precision. *Nature* **331,** 450–453.